Performance of basic mixed oxides for aqueous-phase 5-hydroxymethylfurfural-acetone aldol condensation

Jennifer Cueto, Laura Faba, Eva Díaz, Salvador Ordóñez *

Department of Chemical and Environmental Engineering, University of Oviedo, Julián Clavería s/n, 33006 Oviedo, Spain

ABSTRACT

This paper is focused on the study of the catalytic activity of MgAl and MgZr mixed oxides in the aqueous-phase aldol-condensation of 5-hydroxymethylfurfural (5-HMF) and acetone. The experiment is carried out in a stirred batch reactor. It considers the effect of reaction conditions (namely temperature, reactant concentration and catalyst loading) on catalyst performance. It also looks into the stability of the materials (catalyst reusability in subsequent reaction cycles), as well as into the development and validation of a simplified kinetic model. MgZr catalyst provides the best yield to aldol condensation products, especially for the formation of the second adduct (C15). This material high activity results from its optimum acid/basic sites ratio, mainly medium-strength. Retroaldolization, promoted by stronger basic sites, was identified as an important side-reaction, whereas adsorption effects and oligomerization reactions (evaluated using thermogravimetric analysis and temperature-programmed oxidation of the spent catalysts) determine catalyst stability. Concerning the effect of operation conditions, the best results were obtained working with 0.5 g of MgZr, at 323 K. The highest C15 yield was reached with 5-HMF excess (2:1) (16.1%), whereas the whole yield is maximized at equimolar conditions (37%).

© 2016 Elsevier B.V. All rights reserved.

1. Introduction

The development of processes for obtaining liquid fuels from biomass (especially waste biomass) is nowadays a major challenge. This is due both to environmental reasons (global climate change mitigation) and socio-economical ones (decreasing dependence on oil resources) [1,2]. Considering the different available alternatives, the aqueous phase transformation of lignocellulosic waste biomass is one of the most promising technologies for manufacturing renewable drop-in diesel fuels [3,4]. Mild reaction conditions enhance the interest of this alternative, firstly suggested in 2005 by Dumesic et al. [5]. Substantial research has gone through the different steps of this process, the main issue being at present the development of active, selective, stable and cheap heterogeneous catalysts.

With a view to solving this problem, hemicellulose and cellulose fractions are firstly hydrolyzed into sugars (glucose, xylose, etc.) and dehydrated yielding C5 and C6 aldehydes (mainly furfural and 5-HMF, from C5 and C6 sugars, respectively). This step was taken by using either homogeneous or heterogeneous catalysts, highlighting

the results with acid ones such as MCM-48, Ru-MCM-48, β-zeolites or carbonaceous materials [6–9]. The resulting aldehydes are interesting as bio-platform molecules but they cannot be transformed into valuable fuels by direct hydrogenation, since the resulting hydrocarbons (hexane and pentane) are not appropriate as drop-in petrol (low octane rate) [10,11]. As consequence, increasing the carbon chain length becomes necessary, aldol condensation with acetone (linking molecule) emerging as the easiest option [12]. This reaction yields condensation adducts that can be converted into diesel-quality fuels by a total hydrodeoxygenation [13,14]. Aldol condensation is the key stage in the process, the quality of the final product being directly conditioned by the efficiency of this reaction. As a consequence, this stage has become a crucial object of interest. [15–18]. Optimization using both homogeneous NaOH [19] and heterogeneous materials provided remarkable results with mixed metal oxides [15,20]. After complete hydrogenation and deoxygenation of the condensation adduct, a mixture of linear, diesel-quality alkanes, were obtained.

Although the initial process was carried out on the basis of the valorization of 5-HMF [5], further studies have mainly focused on furfural upgrading [15,17–19]. In principle, the 5-HMF value should be more promising than furfural upgrading, because this aldehyde is obtained from the hexoses, the predominant constituent of lignocellulosic biomass [21]. The 5-HMF valorization has been

Table 1
Summary of the main morphological and chemical properties of the catalysts used in this work.

Catalyst	N_2 physisorption			CO_2-TPD (μmol/g, (K))			NaOH consumption (cm^3/g)	NH_3-TPD (μmol/g)		
	S_{BET} (m^2/g)	dp (nm)	v_p (cm^3/g)	Weak	Medium	Strong		Weak	Medium	Strong
MgAl	237	10.5	0.62	49.7 (340)	71.7 (400)	238.6 (630, 670, 800)	253.2	11.3 (345, 370)	12.5 (450)	41.8 (630, 800)
MgZr	74	10.8	0.82	–	103.4 (400, 450)	52.5 (627)	1.8	52 (360)	41.3 (440)	47.2 (630, 750)

studied as a suitable chemical precursor and also as a monomer for high added value polymers [22]. However, studies about its value for fuel manufacture are rather scarce, most of them focusing on its transformation via etherification with ethanol to obtain compounds with similar energy density as that of mineral gasoline [23,24]. Concerning the 5-HMF upgrading via aldol condensation, *Shen* et al. compared condensation in propanal or acetone and both aldehydes (furfural and 5-HMF) at 393 K using MgZr mixed oxides and NaY [25]. The results obtained show that, despite the higher temperatures, selectivity ratios are significantly lower than those obtained from furfural. Besides, when condensation was studied with acetone, conversion never reached values higher than 50%, much lower than those previously reported in connection with furfural [15,26]. Higher conversion values were reported by *Pupovac* et al., using different spinels as catalysts [27]. However, the experimental conditions of this study (using acetone as solvent and not only as reactant, with higher than 400 K temperatures) were far from those optimized for furfural-acetone condensation, closer to room conditions. Those studies suggest that 5-HMF condensation is more complex than furfural condensation. To the best of our knowledge, this worst behavior has been neither explained nor identified, and a systematic kinetic and deactivation study is yet to be carried out. Consequently, a thorough study of this reaction is required with a view to identifying the catalyst and the reaction conditions that ensure proper conversion, selectivity and stability for the reaction.

This work therefore focuses on the study of aldol condensation of 5-HMF and acetone in aqueous phase. Considering the good results obtained with mixed oxides in aldol condensation of furfural and acetone [15,28], these materials are tested in this reaction (full conversion in less than 12 h and similar product yields, higher than 74% if both products are considered together, with 60 and 43% C13 yield with MgZr and MgAl, respectively [15]). In order to carefully analyze the reaction mechanism, different parameters have been optimized: reaction temperature, catalyst weight, and initial reactant concentration. Reaction data have been correlated with catalysts physico-chemical properties, proposing and experimentally validating kinetics models. Catalyst stability under these conditions has also been studied, the catalysts being reused in subsequent reaction cycles.

2. Experimental and materials

2.1. Catalysts preparation and characterization

MgAl mixed oxide with Mg/Al ratio of 3 was prepared by co-precipitation at low super-saturation conditions (constant pH at 10) under sonication using nitrate salts for each metal. MgZr mixed oxide with a Mg/Zr ratio of 4 was synthesized using the sol-gel technique, solving nitrate salts in deionized water and causing the precipitation by adding NaOH until pH 10. The resulting gel was aged for 24 h. Both mixed oxides were washed with deionized water until pH 7 and then they were isolated by centrifuging. The solids obtained were dried at 393 K for 24 h. Mixed oxides were obtained after heat treatment: in air flow until 973 K in the case of MgAl and in He flow until 873 K in the case of MgZr. In both cases, the

temperature was increased with a 5 K/min ramp and was then held for 3 and 5 h, respectively.

Fresh catalysts were analyzed using different techniques in order to study their surface, morphological and physico-chemical properties and to use these data to identify the main properties affecting catalytic activity. The crystallographic structures were determined by XRD. N_2 physisorption was used to determine the textural characteristics of specific surface area and pore volume. The strength and distribution of basic and acid sites were determined by temperature programmed desorption (TPD) using CO_2 and NH_3 as probe molecules, respectively. ICP-MS and XPS techniques were used to identify the bulk and surface composition. The tools used, as well as the details of each analysis, were mentioned in previous work [15,28,29]. All the characterization results have been studied in detail therein and consequently, they are not included in this paper [15]. Nonetheless, Table 1 summarizes the results and the main parameters mentioned in the discussion.

2.2. Reaction system and procedure

Reactions were carried out in a 0.5 L stirred batch autoclave reactor equipped with a PID temperature controller and a back pressure regulator (Autoclave Engineers EZE Seal). The reactor was loaded with 0.25 L of an aqueous solution of 5-HMF (Sigma Aldrich, 99%) and acetone (Panreac, 99.5%), all of that resulting in an aqueous solution with 2.5% organic compounds. The 5-HMF:Ace initial ratio was 1:1, except in experiments focused on studying the effect, or the reactant concentration ratio. The mixture was heated up to reaction temperature. Under these conditions, the catalyst was added (0.5 g, average diameter of 50–80 μm). The air was purged with N_2 and condensation was carried out under 10 bar of N_2 with a stirring of 1000 rpm for 24 h. These conditions were chosen in order to discard the presence of mass-transfer effects and to guarantee kinetic control. The absence of these mass transfer effects has been tested in previous works for furfural-acetone condensation reaction (a faster reaction) [15]. A blank experiment (reaction without catalyst) discarded any conversion or degradation of any reactant at reaction conditions.

Samples taken from the sampling port were filtered, extracted in ethyl acetate (volume ratio of 1:1) and analyzed by GC in a Shimadzu GC-2010 equipped with a FID detector, using a 30 m long CP-Sil 8 CB capillary column. Peak assignment was performed by GC–MS in a Shimadzu GC/MS QP2010 Plus instrument, using a 30 m long TRB-5MS capillary column. Calibration of condensation adducts (C9 and C15 condensation adducts are not commercially available) was carried out using the Response Factor Method [30]. Once the concentration of each compound was obtained, the evolution of the reaction was studied considering the atomic yield concept, defined as follows:

$$\Psi_{C9}\% = \frac{9 \, mol \, C9}{6 mol \, C6_{t=0} + 3 mol \, C3_{t=0}} \cdot 100 \qquad (1)$$

$$\Psi_{C15}\% = \frac{15 \, mol \, C15}{6 \, mol \, C6_{t=0} + 3 \, mol \, C3_{t=0}} \cdot 100 \qquad (2)$$

Atomic carbon balance was used in order to determine the percentage of reaction compounds that remain soluble in the liquid

phase. Final carbon balance was calculated considering the concentration of each product weight multiplied by the number of carbon in each molecule:

$$C.B._{liqphase}(\%)$$
$$= \frac{3\,molC3 + 6\,molC6 + 9\,molC9 + 15\,molC15}{6\,molC6_{t=0} + 3\,molC3_{t=0}} \cdot 100 \qquad (3)$$

Solids obtained after 24 h reaction were homogenized by mechanical mixture (in order to guarantee the homogeneity of the solids) and analyzed in a TG-DSC instrument (Setaram, Sensys) using α-alumina as inert reference material. Samples (20 mg) were treated in a nitrogen flow (20 mL/min) with a temperature program of 5 K/min from 298 to 973 K. Each sample was analyzed three times in order to guarantee the quantitative character of the results. Considering the amount of solid obtained, TG results were used to complete the carbon balance obtained at the end of the reaction, including the C9 and C15 amount found in the solids and to identify possible volatile oligomerization products:

$$C.B._{react}(\%)$$
$$= \frac{3\,molC3 + 6\,molC6 + 9\,molC9_{liq} + 9\,molC9_{TG} + 15\,molC15_{liq} + 15\,molC15_{TG}}{6\,molC6_{t=0} + 3\,molC3_{t=0}}$$
$$\cdot 100 \qquad (4)$$

The full oxidation of carbonaceous deposits was studied through TPO (temperature programmed oxidation) of the solids obtained at the end of the reaction (after the appropriate mechanical homogenization), using a Micromeritics TPD/TPR 2900. Samples (20 mg) were treated in oxygen flow (2% O_2 in He), increasing the temperature up to 1273 K at a rate of 2.5 K/min while the evolution of CO_2 signal was measured with a mass spectrometer. TPO of the fresh catalysts discarded any contribution of catalyst decomposition. The CO_2 areas obtained were related to results of elemental analyses of these solids (measured in an Elemental Vario EL), obtaining the amount of carbon in the whole solid. The percentage of carbonaceous deposits obtained at the end of each reaction was calculated as the difference between the full carbon balance (C.B.$_{full}$) and the carbon balance of the reaction (C.B.$_{react}$):

$$C.B._{full}(\%)$$
$$= \frac{3\,molC3 + 6\,molC6 + 9\,molC9_{liq} + 15\,molC15_{liq} + molC_{TPO}}{6\,molC6_{t=0} + 3\,molC3_{t=0}}$$
$$\cdot 100 \qquad (5)$$

$$Coke(\%) = C.B._{full}(\%) - C.B._{react}(\%) \qquad (6)$$

3. Results and discussion

3.1. Catalyst performance with equimolar 5-HMF-acetone mixtures

Fig. 1 shows temporary profiles of reactant and product concentrations for the two studied catalysts when reaction was carried out at 323 K. For both catalysts, an initial decrease in the 5-HMF and acetone concentrations, not corresponding to the appearance of any reaction product, has been observed. This fact suggests an initial adsorption of these compounds on the catalytic surface. This fact is congruent with the observed carbon balance evolution: there is an initial decrease of 10% in the first 20 min reaction time, whereas the evolution for longer time is much softer. It is important to highlight that no side-products were detected in the liquid phase analyses, contrary to furfural-acetone condensation, where acetone
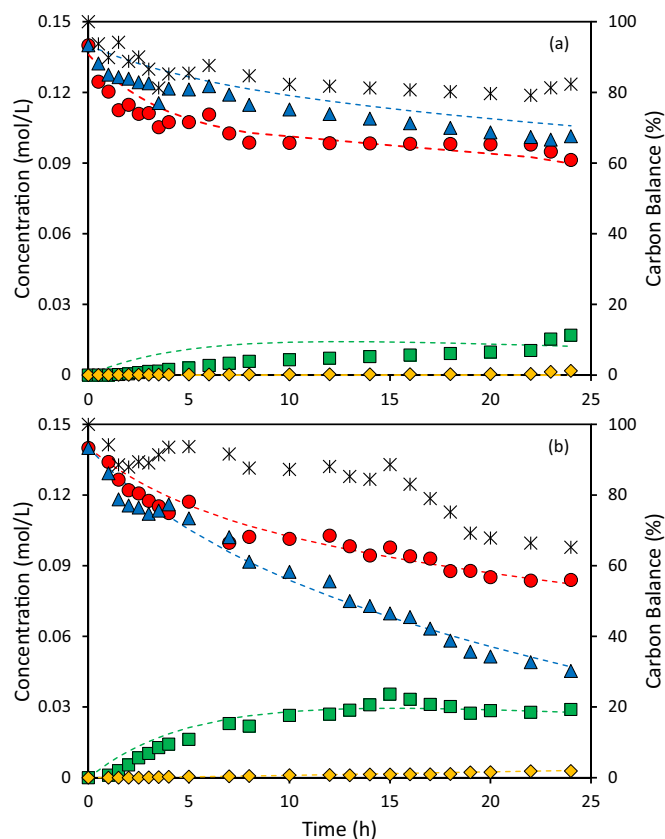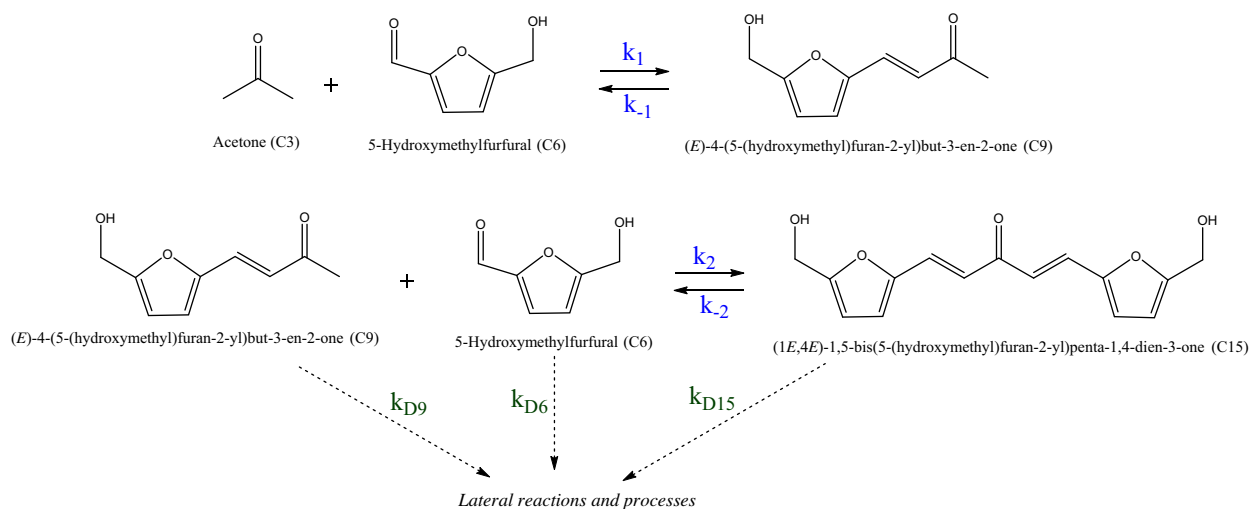

Fig. 1. Temporal evolution of the different reaction compounds involved in the 5-HMF and acetone aldol condensation at 323 K catalyzed by (a) MgAl; (b) MgZr. Symbols: (●) acetone; (▲) 5-HMF; (■) C9; (◆) C15; (✱) carbon balance. Broken lines corresponds to kinetic model predictions.

self-condensation was also observed [15]. This result suggests a stronger adsorption of 5-HMF on catalysts surface, decreasing the acetone surface concentration, and preventing self-condensation.

In general terms, MgZr catalyst is the most active, showing higher conversion for both reactants. In good agreement with the expected reaction scheme (Scheme 1), two products were observed: the first condensation adduct (labelled C9) and the second one (labelled C15), obtained from the reaction of C9 with a second 5-HMF molecule. The last one was only observed in the liquid phase when MgZr is used (3%), whereas only C9 signals were detected for MgAl, with a final C9 yield of 12%. Likewise, a parallel evolution of both reactants was observed with the MgAl catalyst (C9 is a product obtained with an equimolar stoichiometry), obtaining final conversions of 27% and 32% for HMF and acetone, respectively. The carbon balance value obtained after 24 h reaction time was slightly higher than 84%.

On the other hand, when reaction is catalyzed by MgZr mixed oxide, the conversion of 5-HMF (68% at 24 h) was considerably higher than the acetone one (53% at same time), indicating a higher dimmer production. It highlights the low concentration of C15 observed in the liquid phase (3%), despite the high C6 conversion. These results, as well as the decreasing evolution of the carbon balance and the formation of a solid phase, may be due to different reasons: solubility problems of C15 adduct in the aqueous phase, an irreversible adsorption of condensation adducts on the catalytic surface, or the presence of C15 oligomerization side-reactions. Solubility limitations are discarded by calculating the water solubility of both condensation adducts (C9 and C15) using the empirical method proposed by Meylan and co-workers [31]. The suitability of this model was checked by comparing the theoretical and the

Acetone (C3)　+　5-Hydroxymethylfurfural (C6)　$\xrightleftharpoons[k_{-1}]{k_1}$　(E)-4-(5-(hydroxymethyl)furan-2-yl)but-3-en-2-one (C9)

(E)-4-(5-(hydroxymethyl)furan-2-yl)but-3-en-2-one (C9)　+　5-Hydroxymethylfurfural (C6)　$\xrightleftharpoons[k_{-2}]{k_2}$　(1E,4E)-1,5-bis(5-(hydroxymethyl)furan-2-yl)penta-1,4-dien-3-one (C15)

k_{D9}　k_{D6}　k_{D15}

Lateral reactions and processes

Scheme 1. : Proposed reaction network for the aldol condensation of 5-HMF and acetone.

real values of commercial furanyl compounds (furfural and 5-HMF), obtaining a discrepancy lower than 0.5%. According to this methodology, the water solubility of C15 at 323 K is 0.0349 mol/L, more than ten times higher than the maximum concentration observed in the liquid phase (0.0029 mol/L). For the case of C9 adduct, the theoretical solubility is 1.3 mol/L, discarding any solubility problem related to these adducts. In fact, solubility limitations were not observed in the condensation of furfural and acetone, despite the fact that the water solubility of these condensation adducts was significantly lower (0.06 and 0.002 mol/L, for C8 and C13, respectively). Consequently, there is no reason to consider the precipitation of condensation compounds as the main reason for the solid phase formation working at these reaction conditions.

In order to verify the possible presence of reactants, products or oligomers adsorption or even the product precipitation, solid samples recovered after reaction (24 h reaction time in all cases) were homogenized, dried and characterized by thermogravimetry in an inert gas flow. The weight loss evolution with temperature is plotted in Fig. 2a for both catalysts. In the thermogram of MgZr, in addition to the slight decrease observed at temperatures lower than 400 K (associated with water), two main peaks were observed, the first one at 522 K and the second and most important one at 700 K. These temperatures, according to data predicted with *ChemDraw* software and corroborated by Stein and Brown's improved empiric method [32], correspond to boiling temperatures of C9 and C15 condensation adducts (523 and 703 K, respectively).

After 24 h reaction time in using MgAl mixed oxides as catalyst, the amount of solid recovered is significantly lower than that obtained with MgZr but the TG profiles were quite similar (Fig. 2a). The peak associated to water is more relevant than in the case of MgZr, but main peaks also correspond to both C9 and C15 product. Slight differences in the temperatures in dTG lines may be justified by the different isomers that can be obtained in high amount with each material. Considering the presence of linear C=C double bonds, there are two stereoisomers of the first condensation adduct (cis and trans) and three of the second one (double cis, cis-trans and double trans). All these stereoisomers were quantified together in the analytical results for a better understanding, but they can be clearly differenciated by GC-FID (different retention times) and TG (slightly different decomposition temperatures). Cis-C9 is the first adduct obtained with both materials (MgAl and MgZr), but the cis/trans distribution for longer periods at longer times strongly depends on the material, the concentration of the cis isomer being almost negligible with MgZr, but relevant with MgAl. The same
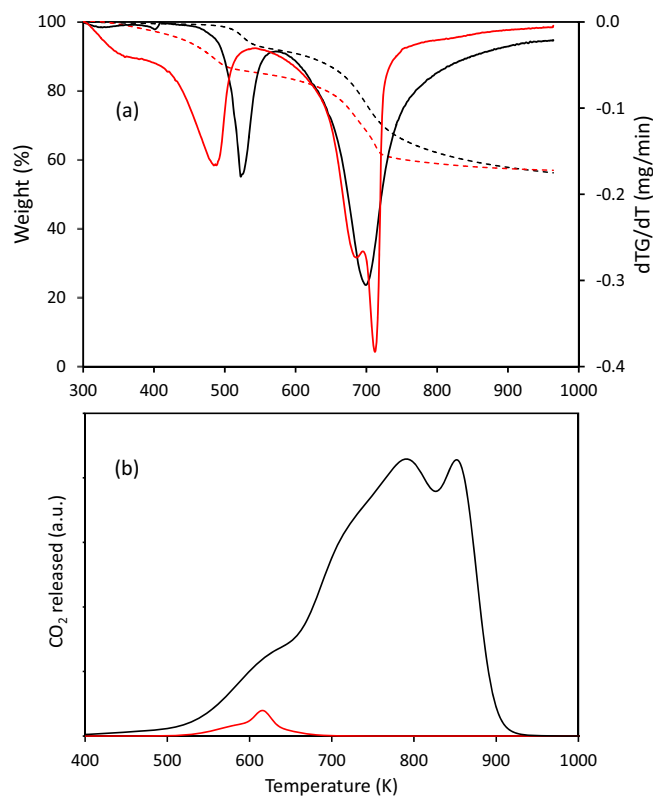

Fig. 2. Analyses of solid phase obtained in the study of the optimum catalyst for the 5-HMF and acetone aldol condensation. (a) Thermogram in nitrogen for the irreversible adsorption of condensation adducts on the catalytic surface; (b) TPO profiles normalized by solid mass analyzed. Codes: MgZr (black), MgAl (red). (For interpretation of the references to colour in this figure legend, the reader is referred to the web version of this article.)

behavior was observed for the second adduct. The double-trans isomers are more stable than the double-cis one, as a result of a more stable electronic distribution. As a consequence, these isomers are more stable and their decomposition temperatures are slightly higher than those of the cis isomers. This discussion is also supported by our previous results in the condensation of furfural and acetone, reaction in which these isomers were identified by NMR [15].

Concerning the comparison in terms of peak areas, the C9/C15 ratio is higher with MgAl. These results confirm the hypothesis that trans-C9 isomer is needed to follow the reaction (interacting with the carbonyl group in the cis isomer involves some limitations). The surface of MgAl, with higher surface area than MgZr and stronger active sites (see Table 1) stabilizes the cis isomer, limiting the activity of this material by surface adsorption. Besides, the small amount of C15 obtained remains adsorbed on the catalytic surface.

The quantification of each mass loss was used to calculate the amount of C9 and C15 present in the solid phase. It must be remarked that, despite the similar profiles obtained in both cases, quantitative results are strongly conditioned by the total amount of solid recovered in each experiment, almost ten times higher in the case of MgZr. These values were added to the final amount observed in the liquid phase after 24 h, considering the equations previously detailed in the experimental section. As for the MgZr, the final concentration obtained for C9 and C15 products was of 0.031 and 0.008 mol/L, respectively.

For this material, final yields after this correction reached values of 22.7 and 14.2% for C9 and C15, whereas the carbon balance increased from 65.2 to 77.1%. This low carbon balance suggests the existence not only of product adsorption but also of a considerable amount of precipitate derived of the condensation adducts oligomerization. Concerning MgAl results, final yields considering the TG and the liquid phase analyses reach values of 13.5 and 5.2%, for C9 and C15, respectively, with a final carbon balance of 88.6%, a good value considering the data reported in the literature for this type of reaction, rarely higher than 80% [20,33].

Comparing the loss of catalyst due to the temperature, highlights the similar final weight that remains after the TG analyses (57% for MgAl and 56.2% for MgZr) despite the fact that the amount of solid recovered with MgZr was 10 times higher than the one obtained with MgAl. This result can be explained considering the maximum temperature reached in these analyses (973 K in inert conditions). At this temperature, possible oligomers precipitated on the MgZr catalytic surface remain in solid state, without obtaining any signal in the TG. These temperatures only produce a partial pyrolysis of these solids, which on its turn explains the continuous decrease in the weight at temperatures higher than 700 K, but their complete decomposition is not possible under these conditions. Consequently the solid recovered after the analysis keeps being brown (whereas the fresh material is white). On the other hand, in the case of MgAl the weight loss percentage keeps constant since the peak corresponding to the C15 signal, so we can work out that all the material deposited on the catalytic surface has been removed and 57% of the initial mass corresponds only with the catalyst (in fact, the solid after the TG analysis has recovered its white color).

This justification is better explained considering the significant differences in the TPO analyses of both spent catalysts, Fig. 2b. According to the data predicted by the ChemDraw software, the combustion temperatures of both products will be 440 and 625 K. In good correspondence with this hypothesis, a relevant peak was observed at 625 K, related to the presence of an important amount of the second condensation adduct. In the case of MgZr, there is also a relevant signal of CO_2 at temperatures over 750 K, 135 mmol CO_2/g_{cat}, which agrees with the hypothesis of an important contribution of oligomerization. This high signal makes it difficult to identify the first condensation peak, which presents much lower concentration. Considering this carbon, the final carbon balance increases to 86.7%. This result corresponds to 9.6% of the initial carbon transformed into non-volatile oligomers. The TPO analysis of MgAl confirms that no side products or oligomers are obtained with this material, only the C9 and C15 signals were observed (no signals were detected over 1000 K). Thus, the carbon balance of MgAl after adding the TPO results only increases from 88.6% to 88.7%.
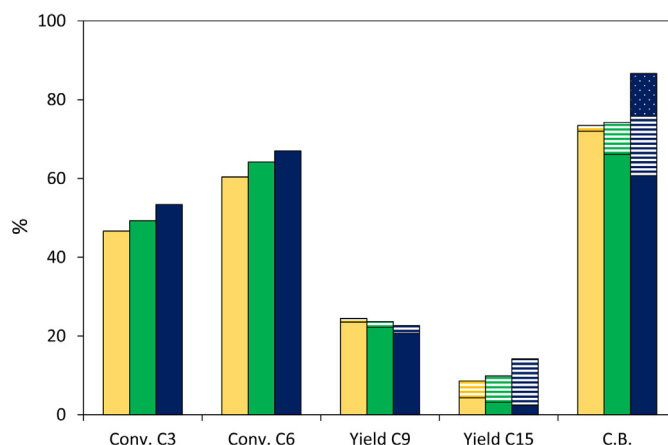

Fig. 3. Summary of results obtained after 24 h of 5-HMF-acetone aldol condensation at 323 K catalyzed by 0.1 g (yellow); 0.25 g (green) or 0.5 g (blue) of MgZr. Results in terms of reactant conversions, product yields and carbon balance. Solid colors correspond to results obtained in the liquid-phase analysis; striped bars correspond to TG analyses and dotted bars indicate the TPO results. (For interpretation of the references to colour in this figure legend, the reader is referred to the web version of this article.)

Reactions were repeated increasing the reaction time in order to determine whether longer times can increase the MgAl activity and also whether MgAl is not active to obtain the second product. After 96 h reaction catalyzed by MgAl, negligible amount of solid oligomers were obtained, suggesting that this active phase is not active for the formation of this material. The 5-HMF conversion obtained with MgAl after this time was 53.8%, with 28.6% of acetone conversion (whereas at 24 h reaction time acetone and 5-HMF conversions were 32 and 27%, respectively), with C9 and C15 yields of 20.2 and 6.6% (12.1 and 1.2% for 24 reaction time), and similar carbon balance (85.6%). When the same procedure was followed with MgZr, the 5-HMF conversion reached 89.3%, with 59.9% of acetone conversion (conversions after 24 h were 53 and 68%, for acetone and 5-HMF, respectively). Once the thermogravimetric results of the solid phase were considered, the final yields obtained with MgZr rose to 13.6 and 25.9%, for C9 and C15 respectively. The carbon balance after 96 h decreased to 59.7% (only 30% when only liquid phase was considered) but this value increased to 87.4% when TPO results were added.

In both cases, the reactants and product concentrations were almost constant along the last 36 h, with no C9 or C15 formation despite the existence of unreacted 5-HMF and acetone. As it is explained in the sections below, the complete deactivation of these materials is discarded, so these results are not related to loss of activity. Taking this fact into account, these results are explained by the existence of retro-aldolization equilibria in both steps of the reaction. These equilibria were previously observed in the furfural-acetone aldol condensation [34]. The comparison of both results suggests that MgAl is not active enough for C15 production, mainly because the reverse reaction in the first step is more relevant than with MgZr. As a consequence, MgZr is proposed as the most active material (higher conversion and higher C15 yield).

3.2. Influence of catalyst loading on reactor performance

In order to further understand the role of the catalytic surface in this reaction, additional experiments were performed varying the amount of catalyst. These experiments may help to highlight the relevance of surface phenomena such as adsorption and may have a key role in the verification of the kinetic model proposed in the following section. Fig. 3 shows results obtained in terms of reactant conversion, atomic yield of the different fractions, and carbon
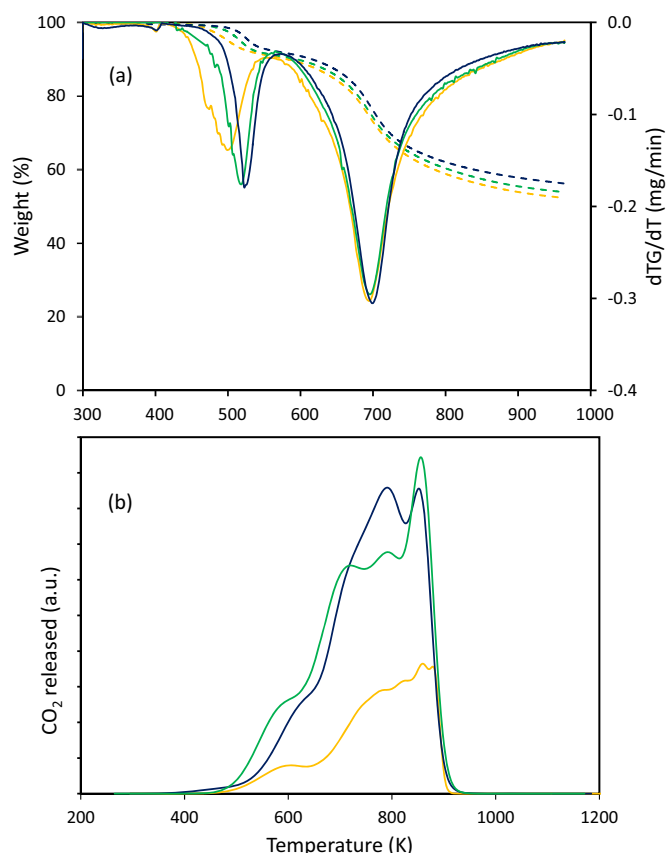
Fig. 4. TG and TPO analyses of solid phase obtained in the study of the influence of catalytic loading in the condensation catalyzed by MgZr: (a) Thermogram for the irreversible adsorption of condensation adducts on the catalytic surface; (b) TPO profiles normalized by solid mass analyzed. Codes: 0.1 g (yellow); 0.25 g (green) or 0.5 g (blue) of MgZr. (For interpretation of the references to colour in this figure legend, the reader is referred to the web version of this article.)

Fig. 5. Summary of results obtained after 24 h of 5-HMF and acetone aldol condensation catalyzed by 0.5 g of MgZr at 303 K (light red); 323 K (medium red) or 343 K (dark red). Solid colors correspond to results obtained in the liquid-phase analysis; striped bars correspond to TG analyses and dotted bars indicate the TPO results. (For interpretation of the references to colour in this figure legend, the reader is referred to the web version of this article.)

balance closures, after 24 h of reaction at 323 K with 0.5, 0.25 and 0.1 g of MgZr. In this figure, results of TG (striped bar) and TPO (dotted bar) analyses are also plotted. As expected, conversions of both reactants increases as catalyst load increases (up to a 10%). However, the evolution of C9 and C15 does not follow an evident trend. Considering concentrations in the aqueous phase, a decrease in the selectivity for both condensation adducts is observed as catalyst weight increases. These yields reached values of 23.5 and 4.3% of C9 and C15, respectively, with 0.1 g of catalyst, whereas only 2.5% of C15 was observed in the liquid phase working with 0.5 g of MgZr. However, the final results when the amount of adsorbed/solid products were considered (TG results) are the opposite, mainly in the case of C15 (a most interesting product), as may be observed in Fig. 4a. Comparing results in both phases, we can conclude that the effect of catalytic loading is nearly negligible for the first condensation, with 21–24% of final yield and almost null adsorption in all cases. However, with 0.5 g of MgZr, the final C15 increases from 2.5 to 14.2% when both phases are considered, whereas less than 9% was obtained in the other cases. These results are justified by the lower reaction rate of the second condensation reaction that makes this reaction more sensitive to catalyst loading. On the other hand, adsorption seems to depend mainly on the exposed surface area. Therefore, although the concentration of adsorbed adduct is rather similar in the three cases (Fig. 4a), the relative importance of this adsorption increases as the catalyst load also increases.

If the TPO of the catalysts used is considered (Fig. 4b), we observe that the amount of insoluble organic deposits is largely lower for the experiment performed with 0.1 g of catalyst. Concerning the
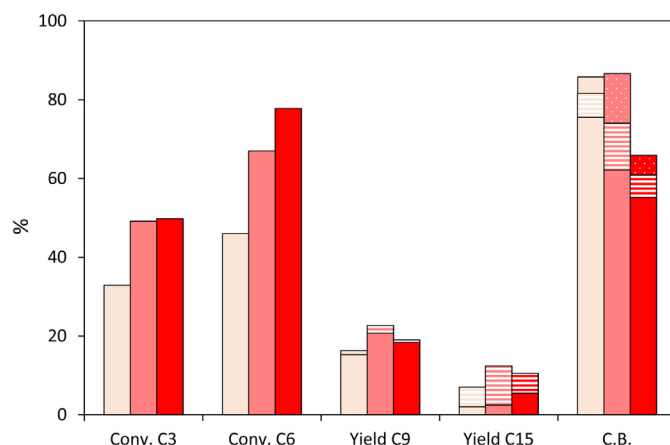
temperatures, they are very similar in both, TPO and TG analyses, for the three samples. Therefore, the different behavior of the lowest catalyst loading is explained by considering that this loading is too low for catalyzing the oligomerization reactions leading to these insoluble deposits.

3.3. Influence of temperature on reactor performance

As consequence of these results, further studies tried to identify the effect of the reaction temperature on catalyst performance. The aldol condensation was studied with 0.5 g of Mg-Zr at different temperatures, Fig. 5. The 303 K temperature was studied with the aim of observing whether lower temperatures can minimize the formation of side and adsorbed products, as previous experiments suggested. Lower temperatures (not shown here) were also tested without observing any relevant conversion. This behavior was previously observed in other condensations of similar biomass-derived compounds [36,37]. On the other hand, temperatures higher than 343 K were discarded because they are too high to allow for the consideration the process as an environmentally-friendly reaction. As it could be expected, the reactant conversions increase at increasing temperatures, this being more pronounced in the case of 5-HMF. Thus, acetone conversion increases from 32.9 to 49.8% when temperature rises from 303 to 343 K. At the same temperature range, the 5-HMF conversion increases from 45.9 to 77.8%. However, these conversions are not related to a similar increase in the product yields. In the case of the C9, there is less than 3% difference between the results obtained at 303 K and at 343 K, the maximum obtained working at intermediate conditions (20.7%). The positive effect of temperature is more evident in the case of C15, increasing from 2.0 to 5.5% (from 303 K to 343 K, when considering only liquid phase concentrations). But these values are very low and do not justify the difference in conversions. The main effect of the temperature is related to the carbon balance and to the solid phase obtained after 24 h. The final carbon balance obtained at 343 K (55.2%) is much lower than the value obtained at 303 K (75.6%).

Analyzing the TG results, profiles showed in Fig. 6a, this decrease does not only correspond to C9 and C15 formation. As may be observed, there is a complete correspondence between profiles obtained at 303 and 323 K, the peaks observed being only related to the two condensation adducts. However, in the case of reaction at 343 K, the profile obtained suggests the presence of different isomers and undesired products. Considering quantitative analyses
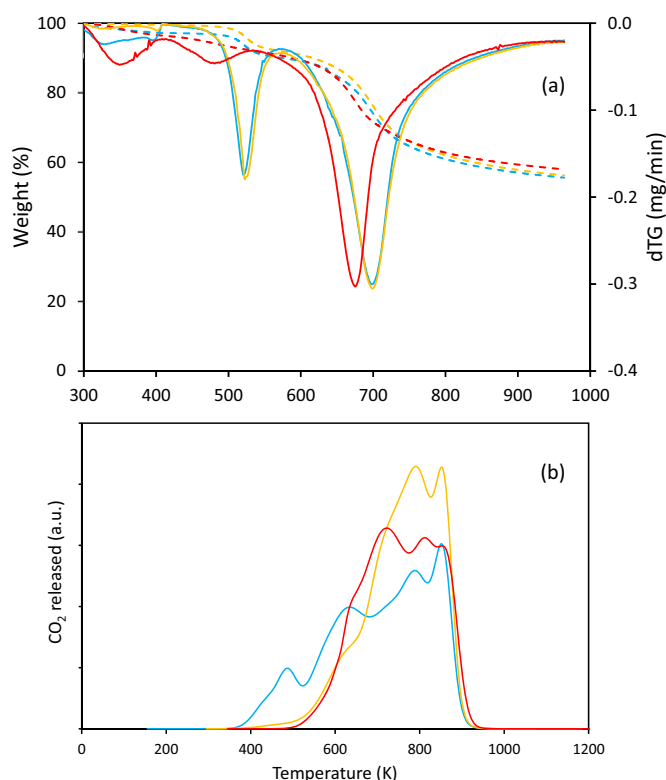
Fig. 6. Analyses of solid phase obtained in the studies of the influence of temperature in the condensation catalyzed by MgZr: (a) Thermogram for the irreversible adsorption of condensation adducts on the catalytic surface; (b) TPO profiles normalized by solid mass analyzed. Reactions carried out using 0.5 g of MgZr as catalyst. Codes: 303 K (blue); 323 K (yellow) and 343 K (red). (For interpretation of the references to colour in this figure legend, the reader is referred to the web version of this article.)

Fig. 7. Summary of results obtained after 24 h of 5-HMF and acetone aldol condensation catalyzed by 0.5 g of MgZr at 323 K using 2:1 (light blue); 1:1 (medium blue) or 1.2 (dark blue) 5-HMF:acetone initial molar ratio. Full colors correspond to results obtained in the liquid-phase analysis; striped bars correspond to TG analyses and dotted bars indicate the TPO results. (For interpretation of the references to colour in this figure legend, the reader is referred to the web version of this article.)

3.4. Influence of reactant ratio on catalyst performance

Results obtained in the previous sections were recorded for experiments performed at equimolar conditions (1:1). Although these conditions have been considered as optimal for cross-condensation of acetone and furfural/5-HMF [15], they mean that reactions are performed under an excess of acetone for the formation of the C15 adduct (Scheme 1). In order to identify the influence of different reactant ratios, experiments were performed working with a constant molar amount of organics, but different acetone/5-HMF ratios. The comparison of final results after 24 h with different reactant ratios at 323 K using 0.5 g of Mg-Zr as catalysts is shown in Fig. 7. As expected, 5-HMF conversion increases as acetone/5-HMF increases, reaching more than 80% at 1:2 conditions. By contrast, the evolution of acetone conversion does not follow clear trends. Concerning the yields to both adducts, C9 yield increases as acetone concentration increases, whereas C15 yield follows the opposite trend (it should be noted that C15 formation requires an excess of 5-HMF). These results are irrespective of considering only an aqueous phase or both phases.

The analysis of TG and TPO results depicted in Fig. 8 highlights the differences observed in the catalyst performance. Concerning the TG analyses (Fig. 8a), an excess of acetone has a positive effect in both C9 and C15 solubility: there is no signal of C9 and the area of the C15 signal is smaller than the area of the other analyses, and its desorption takes place at lower temperatures, suggesting an interaction between C15 and the acetone that modifies the adsorption of the last one. As consequence, TPO analysis of spent catalyst obtained working at 1:2 conditions (acetone excess) (Fig. 8b) shows only a small peak at medium temperatures (580 K), indicating that no oligomers are obtained under these conditions. The low value of final carbon balance obtained even when the solid phase is considered (78.2%) can be due to side reactions of 5-HMF oligomerization without involving acetone.

On the other hand, when there is an excess of 5-HMF in the medium (2:1 conditions, theoretical stoichiometric ratio to C15 formation) the behavior is very similar to that under equimolar conditions (1:1), quite similar profiles in TG and TPO analyses being obtained (Fig. 8b). Results after 24 h when TG analyses are also considered, show that the highest C15 yield was obtained working in 5-HMF excess (16.1%), whereas only 6% was obtained in 1:2 (5-HMF:acetone) ratio. However, if both products are considered together, best results are obtained with equimolar conditions,

(stripped bars in the Fig. 5), final yields of both products would reach values of 16.3 and 7.02% for C9 and C15, respectively, in the reaction at 303 K; and 19.0 and 10.5% for C9 and C15, respectively, in the reaction at 343 K. Final values of carbon balance (considering the products in both phases) are 81.6 and 60.9%, at 303 and 343 K, respectively. Considering the TPO results (profiles observed in Fig. 6b and quantitative results overloaded in Fig. 5), high temperature is not directly related to total amount of insoluble organic compounds, the maximum amount of organic insoluble deposits obtained being at 323 K (9.6%). However, it should be noted that both in TG and TPO, the profiles obtained for catalyst used at the highest temperature and for the other two temperatures are clearly different, thus pointing at the unequal chemical nature of these deposits.

In fact, the spent catalyst usually recovers its original white color after TPO analyses, whereas the catalyst obtained in the reaction at 343 K keeps being dark grey, which shows that there are still some oligomeric deposits that were not oxidized at 1000 K. Oxidation at higher temperatures cannot be tested by TPO analyses because there is no guarantee for the stability of the catalytic structure at temperatures over the highest reached in its preparation. These results suggest that reaction at 343 K follows a different mechanism and cannot be considered to optimize C9 and C15 formation. On the other hand, 303 K is too low to be efficient for C15 formation. According to this, 323 K is considered as the optimum temperature to study 5-HMF and acetone aldol condensation, reaching 37% of product yields.
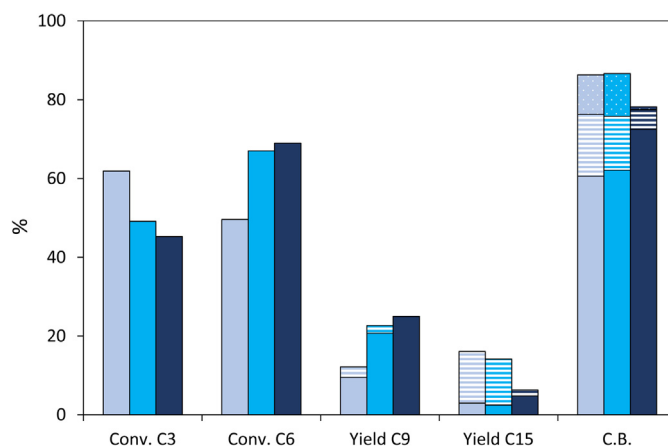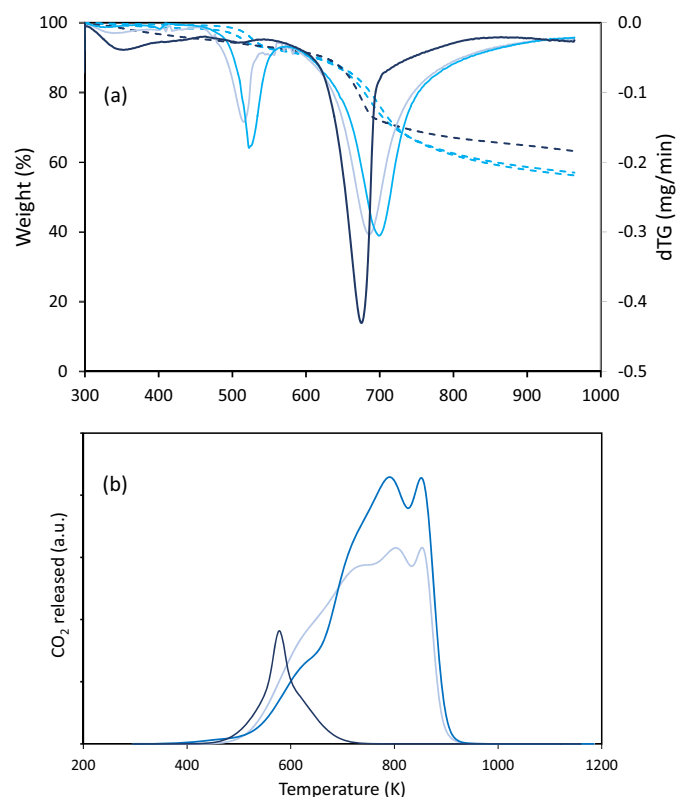
Fig. 8. Analyses of solid phase obtained in the studies of the influence of reagents initial rate in the condensation catalyzed by MgZr at 323 K: (a) Thermogram for the irreversible adsorption of condensation adducts on the catalytic surface; (b) TPO profiles normalized by solid mass analyzed. 5-HMF:acetone reagent rates: 2:1 (light blue); 1:1 (blue) and 1:2 (dark blue). (For interpretation of the references to colour in this figure legend, the reader is referred to the web version of this article.)

reaching 37% of global yield, whereas only 28.3% was obtained with 2:1 conditions. It should be noted that acetone is not the limiting reactant in all the experiments performed. Final carbon balance obtained in the equimolar and 5-HMF acetone excess are very similar (close to 90%), providing around 10% of organic insoluble deposits in both cases. These findings are not conclusive, observing an optimum ratio of commitment by maximum global yield (equimolar conditions) and maximum C15 obtained (5-HMF excess). The results are significantly different from those previously obtained in the condensation of furfural and acetone, in which equimolar conditions are the most favorable to maximize the C13 yield whereas a furfural excess is the best option if both products are considered together [15]. These differences are congruent with the strongest interaction of the 5-HMF with the catalytic surface, in comparison to the case of furfural.

3.5. Catalysts stability

Three general reasons have been previously reported as the main deactivation causes in base-catalyzed reactions: morphological changes on the catalytic surface because of its contact with water, catalyst leaching in aqueous media, and fouling of the catalyst surface by condensation oligomers. ICP-MS of the liquid recovered after 24 h of reaction indicates that there was only 0.89% and 0.005% of Mg and Al, respectively, when MgAl was used; and 1.3% and 0.001% of Mg and Zr in the case of using MgZr as catalyst. Consequently, metal leaching was discarded as main deactivation. Subsequently the homogenously catalyzed reaction can be neglected in the forthcoming kinetic analysis. Therefore, the pH of the solution keeps almost constant during those 24 h, from 4.04 to

3.89 with MgAl and from 4 to 5.5 with MgZr. This negligible lixiviation is relevant taking into account the catalytic synthesis, in which the precursor salts are soluble in water under these pH conditions. However, this phenomenon was also observed in furfural-acetone condensation, indicating a good structure stability of these materials [15]. In order to determine the crystallographic changes of the catalyst upon suspension in water, XRD of fresh materials is compared to the spectra obtained after suspending the catalysts in aqueous solutions for different time periods. To illustrate this, XRD of MgZr after 2 and 24 h in water are attached as Supplementary information (Fig. S5). As can be observed, the ratio brucite/periclase increases upon suspension, but this change is very fast, the profiles of the catalysts suspended 2 and 24 being essentially identical. This fact suggests that the solid reaches fast phase equilibrium in water, remaining unaltered during the whole reaction period.

Considering the high signals obtained in the TPO analyses, there may be some reason to suppose that the deactivation is mainly caused by fouling by solid oligomers. In order to determine the extent of this deactivation, three consecutive tests were carried out. After the first 24 h cycle, the catalyst was recovered by filtration and a new experiment was carried out under the same reaction conditions without any previous treatment to separate the catalyst from the solid phase obtained in the reaction. This procedure was repeated again, obtaining three cycles with the same catalyst. Considering studies previous to this work, the stability study was carried out with both catalysts at 323 K, using 0.5 g of catalyst and with an equimolar initial reactant ratio. The final results obtained after 24 h of each cycle are summarized in Table 2. In general terms, the stability of the MgZr catalyst is largely better than that corresponding to the MgAl catalyst. Thus, after the third cycle, the MgZr catalyst presents more than 60% of the initial activity (considering both 5-HMF and acetone conversion), keeping the C9 yield constant and presenting 50% decrease in C15 yield. By contrast, the Mg-Al catalyst is completely deactivated for 5-HMF acetone condensation. Although the amount of organic solids is largely higher when MgZr is used as a catalyst, the interaction of oligomers with the catalyst surface is stronger in the case of MgAl catalyst, leading to stronger deactivation.

TG obtained after the first and third cycles (the corresponding figure is included in the *Supplementary information* section) were substantially similar, with a similar amount of C15 adsorbed and only a slight increase in the adsorption of C9. This result is congruent with the blockage of some active sites; making the second condensation more difficult because this step needs more free surface to allow for the interaction between C9 and a second 5-HMF molecule. Concerning the XRD patterns of the used catalyst (Fig. S6, Supplementary information), the main peaks found in the fresh catalyst remain in the used catalysts, but a vast amount of peaks appear at low diffraction angles. These diffraction peaks are typical of organic oligomers. TPO profiles are very similar for both samples (solid obtained with MgAl and with MgZr), confirming the absence of new side reactions with partially deactivated catalyst. When solid phase is also considered (adding the results of TG analyses), these final yields increase to 23 and 13.9%, for C9 and C15, respectively.
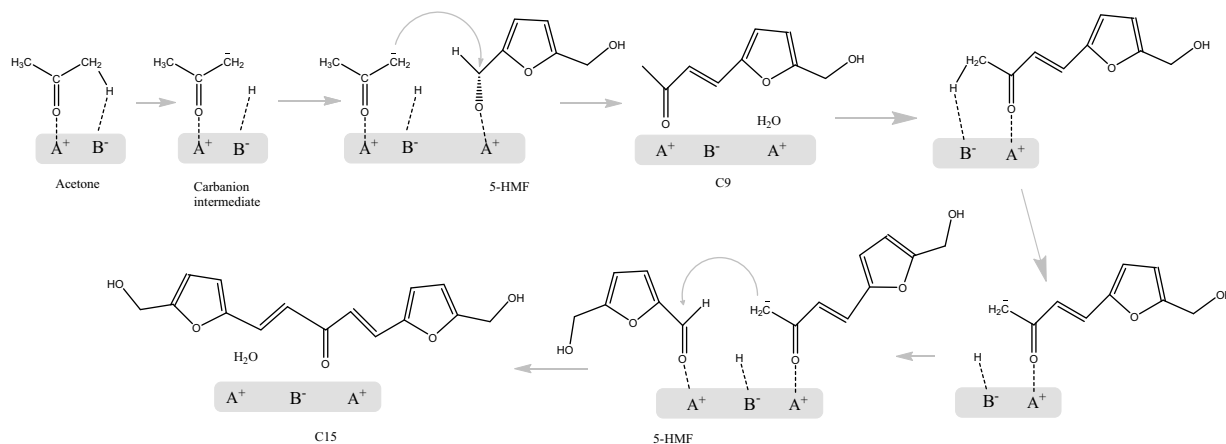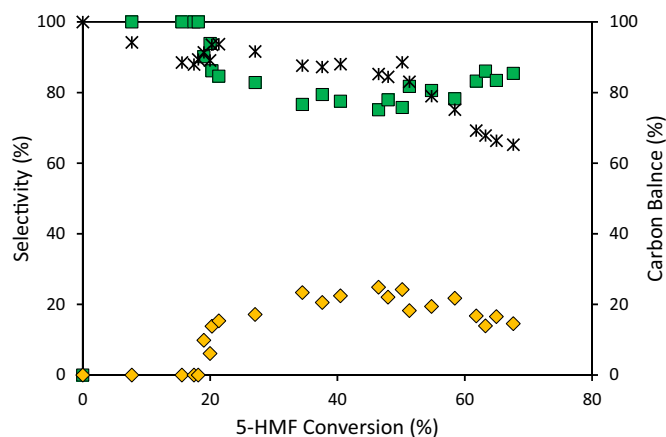
3.6. Reaction mechanism and kinetic modeling

In order to confirm the mechanisms suggested by the temporal evolution of reactions catalyzed by MgZr and MgAl (Fig. 1), Fig. 9 shows the evolution of the different selectivities as a function of 5-HMF conversion, using MgZr as catalyst. According to these profiles (qualitatively similar for all the performed experiments), C9 is identified as the first condensation product, with 100% selectivity at low conversions. 5-HMF conversions higher than 20% are needed to observe the presence of the second product (C15), whose

Table 2
Summary of the final conversions and selectivities obtained in the stability tests of MgAl and MgZr for the 5-HMF and acetone aldol condensation in liquid phase.

| | | Liquid phase analyses | | | | | Solid phase | | | |
| | | Conversion (%) | | Ψ (%) | | Carbon balance (%) | Ψ (%) | | Carbon balance (%) |
		Acetone	5-HMF	C9	C15		C9	C15	
Mg-Zr	1 st cycle	53.4	68.0	20.7	2.9	60.7	22.7	14.2	86.7
	2nd cycle	47.3	51.8	20.4	4.7	77.0	–	–	–
	3rd cycle	33.0	40.2	24.5	1.6	88.4	15.5	9.4	92.7
Mg-Al	1 st cycle	31.8	27.2	12.1	2.1	84.2	13.5	5.2	88.7
	2nd cycle	31.7	10.6	2.2	0	84.0	–	–	–
	3rd cycle	7.5	8.4	0	0	91.8	–	–	–

Scheme 2. Reaction mechanism of the 5-HMF and acetone aldol condensation catalyzed by the studied mixed oxide catalysts.

Fig. 9. Evolution of the main product selectivities as function of the 5-HMF conversion in reaction catalyzed by 0.5 g of MgZr at 323 K. Codes: (■) C9; (♦) C15; (∗) Carbon Balance.

selectivity increases at the same time as the C9 decreases. At the highest conversions, there is a decrease in C15 selectivity justified by both the oligomerization of this compound and retroaldolization reactions (in fact C9 selectivity slightly increases at higher 5-HMF conversions). These evolutions are congruent with the reaction mechanism previously proposed for the aldol condensation of furfural and acetone [15]. This mechanism implies the initial abstraction of one α-proton from acetone, yielding an enolate that attacks the carbonyl group of the 5-HMF molecule. An intermediate β-hydroxyl ketone is obtained but it is not observed because it is not stable under reaction conditions. Consequently, it suffers fast dehydration, obtaining the C9 adduct and regenerating the active sites on the catalytic surface. This product still has an α-proton

that can lead to a second aldolization, obtaining the C15 adduct. This mechanism is sketched in Scheme 2.

According to the proposed mechanism, both C9 and C15 adducts are obtained following a first-order dependence on the concentration of the compound that suffers the enolization (acetone and C9, respectively) and zero-th order dependence on 5-HMF (k_1 and k_2). This zero-th order for the 5-HMF is congruent with a surface process following a Langmuir-Hinshelwood adsorption mechanism, with strong adsorption of the HMF molecule. This hypothesis was previously proposed and corroborated for the aldolization of other bio-platform molecules, such as furfural [11] and citral [35] with acetone, observing in both cases that the condensation takes place with an interaction with a molecule adsorbed on the catalytic surface by its carbonyl group. This adsorption is more relevant with the 5-HMF because of the presence of an extra hydroxyl group that also interacts with the active sites. Both aldol condensation reactions were considered as reversible (k_{-1} and k_{-2}), in good agreement with our results and literature findings. The effect of the adsorption and oligomerization of both condensation adducts, as well as that corresponding to 5-HMF, on the catalytic surface was considered with three more apparent pseudo-first order kinetic constants (k_{D6}, k_{D9}, k_{D15}). Considering both the short reaction times considered in the kinetic model and the low deactivation observed from first to second cycle in the reusability experiments, deactivation kinetics have not been taken into account. Considering these premises, the kinetic model is summarized in the following equations:

$$\frac{d(C3)}{dt} = -k_1 \cdot C3 + k_{-1} \cdot C9 \tag{7}$$

$$\frac{d(C6)}{dt} = -k_{D6} \cdot C6 - k_1 \cdot C3 + k_{-1} \cdot C9 - k_2 \cdot C9 + k_{-2} \cdot C15 \tag{8}$$

$$\frac{d(C9)}{dt} = k_1 \cdot C3 - k_{-1} \cdot C9 - k_2 \cdot C9 + k_{-2} \cdot C15 - k_{D9} \cdot C9 \tag{9}$$

Table 3

Kinetic and adsorption constants for the fitting of the experimental results to the proposed kinetic model when MgAl and MgZr were used as catalyst. In the case of MgZr, the Arrhenius parameters are also detailed. See Scheme 1 to identify the constants.

Catalyst (Temperature)	Kinetic constants (L min^{-1} g^{-1})				Adsorption constants (m^2 min^{-1} g^{-1})			r^2
	k_1	k_2	k_{-1}	k_{-2}	k_{D6}	k_{D9}	k_{D15}	
MgAl (323 K)	0.0443	0	0.1535	0	0	0.6205	0	0.996
MgZr (303 K)	0.0250	0.0074	0.0633	$3.2 \cdot 10^{-11}$	0.0004	0.0003	$1.8 \cdot 10^{-8}$	0.9996
MgZr (323 K)	0.0851	0.0096	0.0919	$1.7 \cdot 10^{-8}$	0.0004	0.0058	$2.9 \cdot 10^{-6}$	0.997
MgZr (343 K)	0.1955	0.0144	0.1045	$2.6 \cdot 10^{-6}$	0.0003	0.0084	$6.1 \cdot 10^{-5}$	0.997
Ea (MgZr) (kJ/mol)	44.6	14.3	71.8	72.8	3.6	10.9	176.9	
k_0	$1.29 \cdot 10^6$	2.11	$8.13 \cdot 10^{10}$	$2.22 \cdot 10^{-5}$	$1.84 \cdot 10^2$	5.04	$1.5 \cdot 10^{-23}$	

$$\frac{d(C15)}{dt} = k_2 \cdot C9 - k_{-2} \cdot C15 - k_{D15} \cdot C15 \quad (10)$$

This kinetic model was checked by fitting the temporal profiles of all the products involved at the reaction conditions studied using the Scientist software. Ideal batch reactor behavior has been considered in all cases. Kinetic data are summarized in Table 3, whereas the value of the model is shown by means of broken lines in Fig. 1 for MgZr and MgAl under standard conditions and in the *Supplementary information* for the other experiments. Kinetic constants have been normalized as function of the catalyst mass. In general terms, very good fitting was obtained for all the compounds. The goodness of this model was backed up when considering the good fitting of reactions at different catalytic loading (the three reactions fit respond to the same kinetic constants). Taking into account the similar morphological parameters of both materials (and their mesoporous character), a different relevance in molecular size limitations is discarded. According to *ChemDraw* software simulation, the molecular diameters are 1.08 and 1.33 nm, for C9 and C15, respectively. These values are one order of magnitude lower than the average pore diameter, discarding diffusion limitations in both cases. Consequently, the different catalytic activity can be only justified by different distribution and concentration of basic and acid sites.

Comparing the kinetic constants obtained for both catalysts, higher values of k_1 and k_2 were obtained for MgZr catalyst, which is in good agreement with its higher concentration of the medium-strength basic sites (Table 1), required for the rate-limiting step of this reaction [15]. These k_1 and k_2 values, as well as the lower values of retroaldolization constants (k_{-1} and k_{-2}) justify the good performance of this material. According to kinetic constants, the first step of aldol condensation is twice slower with MgAl (the concentration of medium-strength basic-acid pairs is almost reduced by half with this material), whereas the second step is almost prevented when this material is used. The lower acidity of the α-proton in C9 justifies that stronger adsorption is needed to produce the proton abstraction. Consequently, the strength of these medium-basic sites must be higher, as in the case of MgZr (the strength of active sites is directly related to the desorption temperature in a TPD).

The lower concentration of medium-strength acid sites observed in the MgAl also justifies the higher relevance of retroaldolization (k_{-1} and k_{-2}), because the dehydration of the intermediate reaction is not fast enough to prevent the reverse reaction [38]. Considering that results of basicity measured in gas phase cannot be conclusive enough, the basicity in aqueous phase was analyzed by suspending a sample of each catalysts in a NaCl solution for 4 h. After this time (sufficient to stabilize the catalytic structure), 5 mL of NaOH 0.1 M was added and the solution was titrated with HCl 0.1 M. The volume used in each analysis is summarized in Table 1, showing that the concentration of Bronsted basic sites of MgZr is two orders of magnitude higher than for the MgAl.

The aldol condensation of 5-HMF and acetone is also influenced by the irreversible adsorption of the aldehyde and both condensation adducts on the catalysts. This adsorption is enhanced by the

hydroxyl groups and their interaction with the strongest acid sites on the catalytic surface [39].

Comparing the kinetic constant values with those previously reported for the furfural − acetone aldol condensation [15], it highlights that a similar k_1/k_{-1} ratio was obtained, despite of the catalyst, indicating a similar activity for the first condensation of both bio-platforms (furfural and 5-HMF). This hypothesis supports the fact that the enolization takes place on the acetone molecule, so the reaction is not directly influenced by the aldehyde, present at high concentration rates on the catalyst surface. In absolute terms, k_1 values are higher in the condensation of furfural than in the condensation of 5-HMF, which is related to higher concentration of active sites for acetone enolization in the former case. With both materials, the first condensation of 5-HMF is much more favored than the second one, being more evident in the case of MgAl (presenting negligible k_2). The opposite behavior was observed for the furfural-acetone aldol condensation, with k_1/k_2 ratios lower than 1 (0.001 and 0.35 for MgAl and MgZr, respectively). These differences can be justified by the stronger adsorption of the first condensation adduct on the catalytic surface due to interaction between the hydroxyl group with the surface.

Kinetic constants at different temperatures were fit according to Arrhenius' theory, obtaining good fittings (the coefficient of determination was higher than 0.9 for all the steps). The activation energy of each step, as well as the values of k_0 are also summarized in Table 3. The activation energy in both equilibrium steps is higher for the inverse reaction, justifying that equilibria of both steps is displaced to a forward reaction. All the values obtained for the direct reactions are congruent with values previously proposed for other cases of condensation of bio-platform molecules [16,28,40] and in good agreement with the theoretical study for the condensation of 5-HMF and acetone reported by Chen et al. [41]. Concerning lateral reactions, C6 and C9 based reactions present low activation energies, suggesting that mainly physical processes (such as adsorption) are involved whereas in the case of C15, the larger activation energy suggests that chemical reactions can have an important weight in this step, most likely oligomerization reactions. This fact is in good agreement with the behavior shown by the catalyst at the highest temperature tested.

4. Conclusions

The liquid phase 5-HMF and acetone aldol condensation was studied using two different mixed oxides. Higher activity, selectivity and stability were obtained with MgZr, but all these results were conditioned by strong adsorption of both condensation adducts (more relevant for MgAl oxides), as well as by the oligomerization reaction of these condensation adducts (more relevant for MgZr). This adsorption controls the whole reaction, being in general less favorable than for furfural-acetone condensation (the other aldehyde obtained from lignocellulosic biomass).

Reaction conditions were optimized, maximizing the product yields when reaction is carried out at 323 K, using 0.5 g of cata-

lyst. Lower temperatures are not enough to activate the catalysts whereas higher temperatures lead to undesired side reactions. The effect of the initial reactant ratio was also studied, being observed that equimolar conditions enhance the global yield but the highest C15 selectivity is obtained in stoichiometric conditions (2:1).

Experimental data was fitted to a reaction mechanism considering two serial reversible first order reactions, and lateral reactions/processes for 5-HMF, C9 and C15 adducts. Concerning the stability of these mixed oxides, three consecutive cycles were tested, obtaining complete activity loss in the case of MgAl and a decrease in conversions below 20% when MgZr was used. The deactivation of these mixed oxides is related to the blockage of the active sites by irreversible adsorption of condensation products, more evident in the case of MgAl.

Acknowledgments

Appendix A. Supplementary data

Supplementary data associated with this article can be found, in the online version, at http://dx.doi.org/10.1016/j.apcatb.2016.08.013.

References

[1] D.M. Alonso, J.Q. Bond, J.A. Dumesic, Green Chem. 12 (2010) 1493–1513.
[2] A. Corma, S. Iborra, A. Velty, Chem. Rev. 107 (2007) 2411–2502.
[3] M. Stocker, Angew. Chem. Int. Edit. 47 (2008) 9200–9211.
[4] G.W. Huber, J.A. Dumesic, Catal. Today 111 (2006) 119–132.
[5] G.W. Huber, J.N. Chheda, C.J. Barrett, J.A. Dumesic, Science 308 (2005) 1446–1450.
[6] A. Toftgaard Pedersen, R. Ringborg, T. Grotkjær, S. Pedersen, J.M. Woodley, Chem. Eng. J. 273 (2015) 455–464.
[7] B.T. Kusema, L. Faba, N. Kumar, P. Mäki-Arvela, E. Díaz, S. Ordóñez, T. Salmi, D.Y. Murzin, Catal. Today 196 (2012) 26–33.
[8] L. Faba, B.T. Kusema, E.V. Murzina, A. Tokarev, N. Kumar, A. Smeds, E. Díaz, S. Ordóñez, P. Mäki-Arvela, S. Willför, T. Salmi, D.Y. Murzin, Microporous Mesoporous Mater. 189 (2014) 189–199.
[9] D.Y. Murzin, E.V. Murzina, A. Tokarev, N.D. Shcherban, J. Wärnå, T. Salmi, Catal. Today 257 (2015) 169–176.
[10] M. Yabushita, H. Kobayashi, A. Fukuoka, Appl. Catal. B 145 (2014) 1–9.
[11] U. Addepally, C. Thulluri, Fuel 159 (2015) 935–942.
[12] N. Qureshi, T.C. Ezeji, Biofuel Bioprod. Biorefin. 2 (2008) 319–330.
[13] L. Faba, E. Díaz, S. Ordóñez, Catal. Sci. Technol. 5 (2015) 1473–1484.
[14] L. Faba, E. Díaz, A. Vega, S. Ordóñez, Catal. Today 269 (2016) 132–139.
[15] L. Faba, E. Díaz, S. Ordóñez, Appl. Catal. B 113–114 (2012) 201–211.
[16] R.E. O'Neill, L. Vanoye, C. De Bellefon, F. Aiouache, Appl. Catal. B 144 (2014) 46–56.
[17] X.-M. Huang, Q. Zhang, T.-j. Wang, Q.-y. Liu, L.-l. Ma, Q. Zhang, J. Fuel Chem. Technol. 40 (2012) 973–978.
[18] O. Kikhtyanin, V. Kelbichova, D. Vitvarova, M. Kubu, D. Kubicka, Catal. Today 227 (2014) 154–162.
[19] R.M. West, Z.Y. Liu, M. Peter, C.A. Gärtner, J.A. Dumesic, J. Mol. Catal. A 296 (2008) 18–27.
[20] C.J. Barret, J.N. Chheda, G.W. Huber, J.A. Dumesic, Appl. Catal. B 66 (2006) 111–118.
[21] Y. Sun, J. Cheng, Bioresour. Technol. 83 (2002) 1–11.
[22] R.J. Putten, J.C. Waal, E. de Jong, C.B. Rasrendra, H.J. Heeres, J.G. Vries, Chem. Rev. 113 (2013) 1499–1597.
[23] P. Lanzafame, D.M. Temi, S. Perathoner, G. Centi, A. Macario, A. Aloise, G. Giordano, Catal. Today 175 (2011) 435–441.
[24] P. Lanzafame, K. Barbera, S. Perathoner, G. Centi, A. Aloise, M. Migliori, A. Macario, J.B. Nagy, G. Giordano, J. Catal. 330 (2015) 558–568.
[25] W. Shen, G.A. Tompsett, K.D. Hammond, R. Xing, F. Dogan, C.P. Grey, W.C. Conner Jr., S.M. Auerbach, G.W. Huber, Appl. Catal. A 392 (2011) 57–68.
[26] L. Hora, V. Kelbichová, O. Kikhtyanin, O. Bortnovskiy, D. Kubicka, Catal. Today 223 (2014) 138–147.
[27] K. Pupovac, R. Palkovits, ChemSusChem 6 (2013) 2103–2110.
[28] L. Faba, E. Díaz, S. Ordóñez, ChemSusChem 6 (2013) 463–473.
[29] L. Faba, E. Díaz, S. Ordóñez, Biomass Bioenergy 56 (2013) 592–599.
[30] J.T. Scalon, D.E. Willis, J. Chromatogr. Sci. 23 (1985) 333–340.
[31] W.M. Meylan, P.H. Howard, S.R. Boethling, Environ. Toxicol. Chem. 15 (1996) 100–106.
[32] S.E. Stein, R.L. Brown, J. Chem. Inf. Comput. Sci. 34 (1994) 581–587.
[33] H. Xiao-Ming, Z. Quing, W. Tie-Jun, L. Qi-Ying, M.A. Long-Iong, Z. Qi, J. Fuel Chem. Technol. 40 (2012) 973–978.
[34] L. Hora, V. Kelbichová, O. Kikhtyanin, O. Bortnovskiy, D. Kubicka, Catal. Today 223 (2014) 138–147.
[35] V.K. Díez, C.R. Apesteguía, J.I. Di Cosimo, J. Catal. 240 (2006) 235–244.
[36] L. Hora, O. Kikhtyanin, L. Capek, O. Bortnovskiy, D. Kubicka, Catal. Today 241 (2015) 221–230.
[37] C. Noda Pérez, C.A. Henriques, O.A.C. Antunes, J.L.F. Monteiro, J. Mol. Catal. 233 (2005) 83–90.
[38] J. Feng, J. Zhu, W. Lv, J. Li, W. Yan, Chem. Eng. J. 269 (2015) 316–322.
[39] S. Sitthisa, T. Sooknoi, Y. Ma, P.B. Balbuena, D.E. Resasco, J. Catal. 277 (2011) 1–13.
[40] O. Casanova, S. Iborra, A. Corma, J. Catal. 265 (2009) 109–116.
[41] S. Chen, H. Yang, C. Hu, Catal. Today 245 (2015) 100–107.